

A Novel Magnetic Nanocatalyst Fe₃O₄@TiO₂-H₅IO₆ for the Green Synthesis of 4-Substituted-1,5-benzodiazepine Derivatives

Fatemeh Ahmadzadeh, Bahador Karami,* Mahnaz Farahi and Jamileh Etemad
Department of Chemistry, Yasouj University, Yasouj, PO Box 353, Iran
karami@yu.ac.ir*

(Received on 6th November 2020, accepted in revised form 18th February 2021)

Summary: In this study, periodic acid-functionalized magnetic support (Fe₃O₄@TiO₂-H₅IO₆) as a new, benign and recyclable nanocatalyst was prepared by anchoring / periodic acid onto TiO₂-coated nano-Fe₃O₄. This catalyst was applied to achieve a high-efficiency, low-cost and eco-friendly approach for synthesizing 4-substituted-1,5-benzodiazepines with the multicomponent reactions of aromatic aldehydes, *o*-phenylenediamine, and dimedone. The / periodic acid group on Fe₃O₄@TiO₂ possesses both Lewis and Brønsted acidity, which is responsible for the high catalyst activity. The obtained results show that the catalyst performance has been acceptable in the presented research. / The catalyst could be recovered and reused up to six times without any notable decrease in its activity.

Key words: Periodic acid; Fe₃O₄; TiO₂; Nanocatalyst; Benzodiazepine.

Introduction

Benzodiazepines are an outstanding class of heterocyclic compounds that find extensive use in pharmaceutical industries [1-3]. They are best known for owning a wide variety of biological properties, including antidepressive [4], antifungal [5], antiepileptic [6, 7], analgesic [8], antibiotic [9, 10], and HIV-1 protease inhibiting activities [11, 12]. Many family members have extensively applied as tranquilizing and anticonvulsant agents [13]. Specifically, 1,5-benzodiazepines, which constitute the fundamental structural units of well-known drugs, are of interest to the medicinal chemist. Its unique central nervous system (CNS) depressant activity made them one of the most widely prescribed psychotropics classes [14]. Fused or functionalized 1,5-benzodiazepines, as useful intermediates, are used to synthesize triazole-, oxadiazole-, oxazino-, and furano-benzodiazepines [15-17]. Most of the synthetic methods reported for the preparation of 1,5-benzodiazepines are related to the reactions of the *o*-phenylenediamine with α,β -unsaturated, carbonyl compounds, β -haloketones, or ketones which some of these processes suffer major or minor restrictions including high catalyst loading, unfavorable product yields, and difficulty in isolation methods of product [18]. Due to the attractive features of 1,5-benzodiazepines, in the present work, we decided to report a comfortable and practical approach for synthesizing them.

Multicomponent reactions (MCRs) are excellent strategies that offer a wide range of advantages, including being quick, simplified, and easy fulfillment, with a high atom economy. So, they have attracted significant interest owing to their impressive synthetic efficiency. Multicomponent reactions have broad applications in medicinal chemistry to produce libraries

of biologically active compounds using readily available starting materials [19-23].

Homogeneous transition metal catalysts often exhibit excellent performance in organic transformations but show drawbacks regarding recovery and recyclability [24, 25]. These kinds of reusable catalysts, such as mesoporous silica or polymers in which transition metal has immobilized / solid supports from industrial and environmental viewpoints, possess many benefits [26]. Much better mild reaction conditions, easy set-up, and work-up are intrinsic features of heterogeneous catalysts over their homogenous analogs. Furthermore, after completing the reaction, the supported catalysts are ready to quickly isolate from the crude mixture through simple filtering or centrifuging and then recovered for more runs. The heterogeneous catalytic systems not only decrease the production of the waste but also show high activity and excellent selectivity [27-31].

Synthesis and applications of nanocatalysts have been undergoing fascinating developments in recent years as a result of their unique chemical and physical properties. The proficiency of nanocatalysts to accelerate the organic reactions and prevent the side routes from obtaining undesired products represents the interest to utilize lower amounts of inexpensive and drastic catalysts [32]. Because of the high surface area and high dispersion of metal nanoparticles (MNPs), they have been used as catalysts in many reactions [33]. The MNP-based catalysts are usually preserved by organic ligands, such as polymers, surfactants, and phosphines, to prevent coalescence. They are used inhomogeneous systems similar to those in which metal-complex catalysts are used [34]. Iron oxide nanoparticles (Fe₃O₄ NPs) are used

*To whom all correspondence should be addressed.

as a practical support for many heterogeneous nanocatalysts owing to their features such as a good imbibition magnetization value, low cost, easy renewability, and recovery by magnetic separation, non-toxicity, and surface changeability [35-38]. These nanoparticles tend to agglomerate to form larger particles. Another limitation of Fe_3O_4 nanoparticles is their sensitivity to oxidation [39]. To inhibit this accumulation and oxidation, a layer is placed on them. In this regard, coatings such as SiO_2 [40, 41], TiO_2 [42-44], graphene, and graphene oxide [45, 46] have been used in various articles recently. In this study, Fe_3O_4 nanoparticles have been coated by a TiO_2 layer to chemically stabilize bare iron oxide nanoparticles against damage during or after the subsequent application. Furthermore, the TiO_2 shell is straightforward to be functionalized and suitable for binding / various catalytic species.

The purpose of this research is to highlight the use of reusable nanocatalysts with inherent magnetic properties for the preparation of some biologically active heterocycles. Herein, in recent analysis [47-58], we prepared a solid acid catalyst via anchoring periodic acid on $\text{Fe}_3\text{O}_4@ \text{TiO}_2$ by a simple procedure whose catalytic activity on the one-pot synthesis of benzodiazepines has been investigated.

Experimental

General materials and instruments

All chemicals used in this research were purchased from Fluka and Merck chemical companies. The monitoring of the reaction progress was accomplished using thin-layer chromatography (TLC) performed with silica gel SIL G/UV254 plates (hexane:EtOAc). Ultrasonic irradiation was performed in an ultrasound cleaning bath KQ-250 DE with a frequency of 40 kHz, and power of 250 W. Melting points were determined by an electrothermal KSB1N apparatus. The NMR spectra of ^1H were recorded in $\text{DMSO}-d_6$ on Bruker Avance UltraShield 400 MHz instrument spectrometers, and ^{13}C NMR spectra were recorded at 100 MHz. Fourier transforms infrared (FT-IR) spectra were obtained with a JASCO FT-IR/680 instrument spectrometer using KBr pellets. X-ray powder diffraction (XRD) patterns were recorded using a Bruker AXS (D8 Advance) X-ray diffractometer with $\text{Cu K}\alpha$ radiation ($\lambda = 0.15418 \text{ nm}$). The measurement was made in 2θ ranging from 10° to 80° at the speed of $0.05^\circ \text{ min}^{-1}$. Energy dispersive spectroscopy (EDS) was obtained using the TESCAN vega model instrument. The particle size and morphology of the particles were studied by scanning electron microscopy (SEM: KYKY-EM3200) experiments under an acceleration voltage of 26 kV. The

magnetic measurement was carried out in a vibrating sample magnetometer (VSM; Kashan University, Kashan, Iran) at room/temperature.

Procedure for the synthesis of Fe_3O_4 NPs

Nano- Fe_3O_4 was fabricated according to a reported method [59]. The mixture of $\text{FeCl}_3 \cdot 6\text{H}_2\text{O}$ (2.7 g, 10 mmol) and $\text{FeCl}_2 \cdot 4\text{H}_2\text{O}$ (1 g, 5 mmol) in distilled water (45 mL) was stirred for 15 min under an argon atmosphere at 80°C . Followed by NaOH solution (5 mL, 10 M) was added drop-wise until the color darkened. The mixture was stirred vigorously for 1 hour and then the attained black products were collected and washed several times with deionized water and ethanol, and then dried at 60°C .

Preparation of $\text{Fe}_3\text{O}_4@ \text{TiO}_2$

The prepared Fe_3O_4 MNPs were dispersed in a mixture of ethanol and acetonitrile (125:45 mL) ultrasonically for 15 min. A particular NH_3 aqueous solution (0.75 mL, 25%) was added to the mixture under stirring. After the continuous mechanical stirring for 30 min, tetraethyl orthotitanate (TEOT) (1.5 mL) dissolved in absolute ethanol (20 mL) was added drop-wise to the above suspension. In the end, $\text{Fe}_3\text{O}_4@ \text{TiO}_2$ was separated by an external magnet, washed/ three times by EtOH, and dried at room/temperature for one day [60].

Synthesis of periodic acid-functionalized magnetic TiO_2 nanoparticles ($\text{Fe}_3\text{O}_4@ \text{TiO}_2@ \text{H}_5\text{IO}_6$)

A mixture of $\text{Fe}_3\text{O}_4@ \text{TiO}_2$ (0.5 g) and H_5IO_6 (2.50 g, 10.96 mmol) in DMSO (15 mL) was stirred at reflux under argon atmosphere for 24 hours. Then, the obtained $\text{Fe}_3\text{O}_4@ \text{TiO}_2@ \text{H}_5\text{IO}_6$ nanocatalyst was filtered and washed two times with ethanol, once with distilled water, and dried at 60°C for 6 hours and dried in the oven at 100°C .

General procedure for the synthesis of 4-substituted-1,5-benzodiazepines

$\text{Fe}_3\text{O}_4@ \text{TiO}_2@ \text{H}_5\text{IO}_6$ (0.002 g) was added to a mixture of aldehyde (1 mmol), *o*-phenylenediamine (1 mmol), and dimedone (1 mmol). The resulting mixture was stirred in an oil bath (80°C) under solvent-free conditions. Stirring was continued till complete conversion was achieved, as confirmed by TLC. When the reaction was finished, the mixture was dissolved in acetonitrile, and the catalyst was separated by an external magnetic field. The loose end solvent vaporized and eventually obtained precipitate was crystallized from hot ethanol.

Spectral data

Compound 5I. Yield 96%; m.p. 278-280 ° C. FT-IR (KBr): ν_{\max} 3465, 3304, 3242, 3114, 2966, 1600, 1415, 1381, 1278, 758 cm^{-1} . ^1H NMR (DMSO- d_6 , 400 MHz) δ = 1.09 (s, 3H), 1.11 (s, 3H), 2.17 (q, 2H, J = 15.1 Hz), 2.65 (s, 2H), 3.35 (s, 1H), 5.42 (d, 1H, J = 7.6 Hz), 5.86 (d, 1H, J = 7.6 Hz), 6.47-7.05 (m, 7H), 8.89 (s, 1H), 10.12 (s, 1H) ppm. ^{13}C NMR (DMSO- d_6 , 100 MHz) δ = 27.60, 29.14, 32.36, 44.54, 49.94, 56.50, 109.09, 109.88, 117.41, 120.41, 120.75, 120.97, 123.29, 129.61, 130.35, 131.44, 133.09, 138.66, 154.97, 156.05, 192.59 ppm. Anal. Calcd. for $\text{C}_{21}\text{H}_{21}\text{BrN}_2\text{O}_2$: C, 61.03; H, 5.12; N, 6.78. Found: C, 61.09; H, 5.10; N, 6.75.

Results and Discussion

The synthetic pathway for the preparation of $\text{Fe}_3\text{O}_4@ \text{TiO}_2\text{-H}_5\text{IO}_6$ magnetic nanocatalyst is shown in Scheme-1. Fe_3O_4 nanoparticles were prepared by chemical coprecipitation of Fe^{2+} and Fe^{3+} ions in a basic solution. Then, the modification of Fe_3O_4 nanoparticles surface was accomplished via a coating layer of TiO_2 employing tetraethyl orthotitanate (TEOT) to obtain $\text{Fe}_3\text{O}_4@ \text{TiO}_2$. Finally, periodic acid can be immobilized on TiO_2 -coated Fe_3O_4 to get our desired magnetic nanocatalyst **1**. Identification and characterization of the physicochemical properties of this catalyst were conducted by applying various analyzes methods such as FT-IR, XRD, FE-SEM, and EDX techniques.

Fig. 1, shows the X-ray diffraction (XRD) patterns of the synthesized $\text{Fe}_3\text{O}_4@ \text{TiO}_2$ and $\text{Fe}_3\text{O}_4@ \text{TiO}_2@ \text{H}_5\text{IO}_6$. As exhibited in Fig. 1 the structure of the crystal is cubic inverse spinel and remains constant after encapsulation and functionalization [61]. In this XRD pattern, the peaks at 2θ values of 30.1, 35.4, 43.05, 57.94, and 62.56 are consistent with the standard XRD data for the structure of Fe_3O_4 , and these peaks are present in two patterns [62]. Moreover, the peaks at 36.4, 53.9, and 63 belong to TiO_2 [63], the two peaks at 36.4 and 63 being overlaid the Fe_3O_4 peaks. According to the Debye-Scherrer equation, the average particle size is estimated at /30 nm.

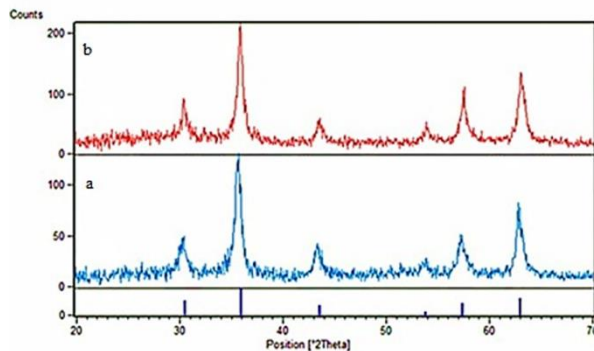


Fig. 1: The XRD pattern of a) $\text{Fe}_3\text{O}_4@ \text{TiO}_2$ and b) $\text{Fe}_3\text{O}_4@ \text{TiO}_2@ \text{H}_5\text{IO}_6$.

The FT-IR spectra of Fe_3O_4 , $\text{Fe}_3\text{O}_4@ \text{TiO}_2$, and $\text{Fe}_3\text{O}_4@ \text{TiO}_2@ \text{H}_5\text{IO}_6$ are demonstrated in Fig. 2. This spectrum helped to confirm the stepwise formation of nanocatalysts. The peak observed at 585 cm^{-1} shows the stretching vibrational modes of Fe-O / are maintained in all samples. In Fig. 2b and 2c, the vibration frequency of Ti-O is located at $500\text{-}600 \text{ cm}^{-1}$ but could not be recognized meticulously due to overlapping with the vibrational stretching of Fe-O in this region. The broad peak in this region in Fig. 1c is related to the O-H stretching vibration of periodic acid. Also, I=O functional groups corresponding to periodic acid have been identified by the appearance of vibrating band at 815 cm^{-1} in Fig. 2c, which is not seen in the two spectrums 2a and 2b and emphasize the stabilization of this acid on the surface of the TiO_2 -coated Fe_3O_4 NPs.

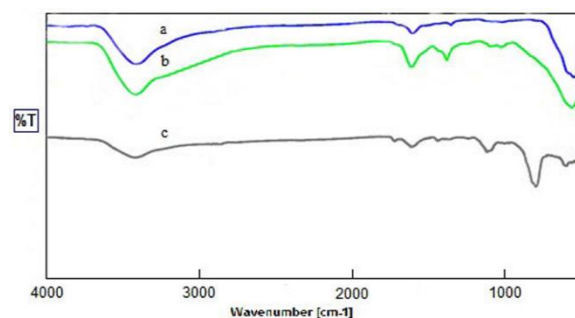
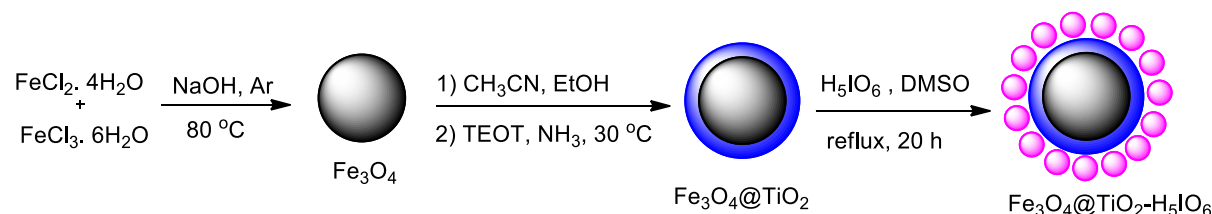


Fig. 2: The FT-IR spectra of a) Fe_3O_4 , b) $\text{Fe}_3\text{O}_4@ \text{TiO}_2$, and c) $\text{Fe}_3\text{O}_4@ \text{TiO}_2\text{-H}_5\text{IO}_6$.



Scheme-1. Preparation of $\text{Fe}_3\text{O}_4@ \text{TiO}_2\text{-H}_5\text{IO}_6$ (**1**).

Energy-dispersive X-ray spectroscopy (EDS) is often used to obtain useful information about the elemental composition of the objects. Herein, the EDS analysis confirmed the presence of Fe, O, Ti, C, H, and I in magnetic nanocatalyst **1**, which guarantees the successful anchoring of periodic acid on $\text{Fe}_3\text{O}_4@ \text{TiO}_2$ (Fig. 3).

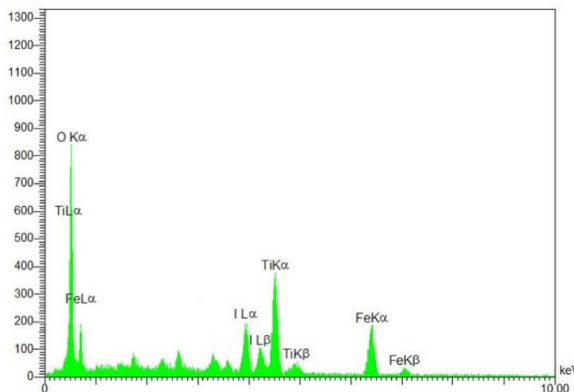


Fig. 3: EDS spectrum of nano $\text{Fe}_3\text{O}_4@ \text{TiO}_2\text{-H}_5\text{IO}_6$.

The morphology of $\text{Fe}_3\text{O}_4@ \text{TiO}_2\text{-H}_5\text{IO}_6$ nanocatalyst was investigated by acquiring a scanning electron microscopy (SEM) image of it, as shown in Fig. 4. The nanoparticles with a narrow distribution of diameters averaging approximately 30 nm were observed in this image.

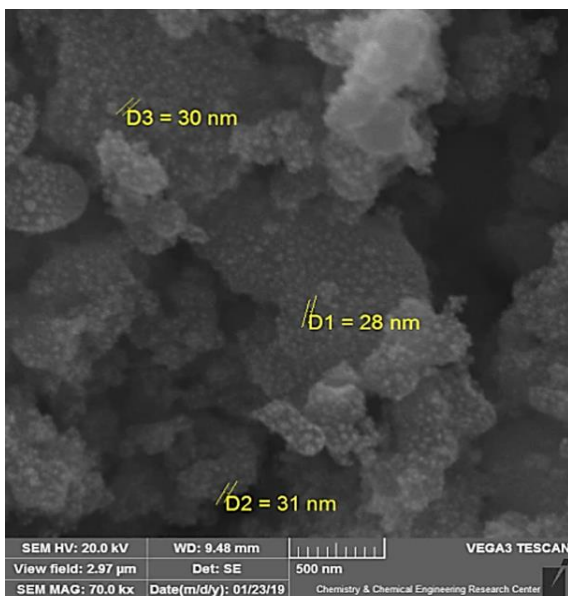


Fig. 4: SEM image of nano $\text{Fe}_3\text{O}_4@ \text{TiO}_2\text{-H}_5\text{IO}_6$.

The below magnetization curves show the saturation magnetization of $\text{Fe}_3\text{O}_4@ \text{TiO}_2$

nanoparticles (Fig. 5a) and $\text{Fe}_3\text{O}_4@ \text{TiO}_2\text{-H}_5\text{IO}_6$ (Fig. 5b), which were reduced to 23 emu g⁻¹ from 70 emu g⁻¹ for $\text{Fe}_3\text{O}_4@ \text{TiO}_2$. As can be seen, the difference in saturation magnetization between $\text{Fe}_3\text{O}_4@ \text{TiO}_2$ nanoparticles and $\text{Fe}_3\text{O}_4@ \text{TiO}_2\text{-H}_5\text{IO}_6$ was small. Despite the reduction in the magnetic value, the catalyst still has a magnetic property and can be easily separated from the reaction by an external magnet.

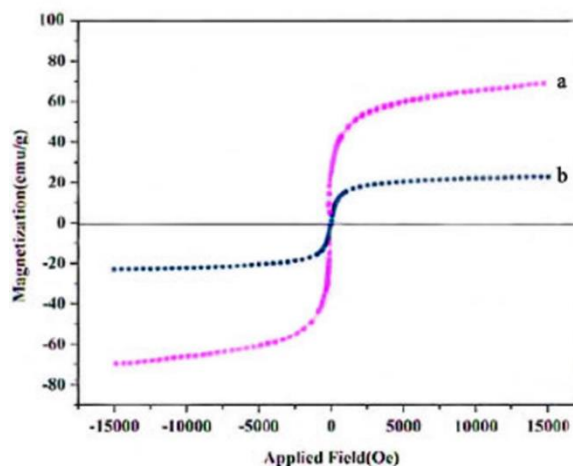


Fig. 5: Room-temperature magnetization curves of a) $\text{Fe}_3\text{O}_4@ \text{TiO}_2$ and b) $\text{Fe}_3\text{O}_4@ \text{TiO}_2\text{-H}_5\text{IO}_6$.

Next, we focused on preparing 4-substituted-1,5-benzodiazepine derivatives **5** by a three-component reaction of *o*-phenylenediamine **2**, dimedone **3**, and aryl aldehydes **4** in the presence of the prepared $\text{Fe}_3\text{O}_4@ \text{TiO}_2\text{-H}_5\text{IO}_6$ (Scheme 2).

Initially, to determine suitable conditions, the reaction of benzaldehyde, *o*-phenylenediamine, and dimedone was selected as a model reaction. The impact of diverse parameters such as the amount of the catalyst, solvent type, and temperature were investigated and optimized (Table-1). Under catalyst and solvent-free conditions at room temperature, we could not obtain the desired product. Next, with increasing the temperature of the reaction, a trace amount of **5a** was obtained. The model reaction was conducted in the presence of various amounts of catalyst **1**. The best yield was obtained in the fact of 0.002 g of catalyst **1**. Investigation of different solvents and reaction temperatures were also done. Subsequently, different amounts of H_5IO_6 were studied. The results of several experimental conditions are summarized in Table-1. Notably, using 0.002 g of $\text{Fe}_3\text{O}_4@ \text{TiO}_2\text{-H}_5\text{IO}_6$ under solvent-free conditions at 80 °C was selected as the optimized reaction conditions.

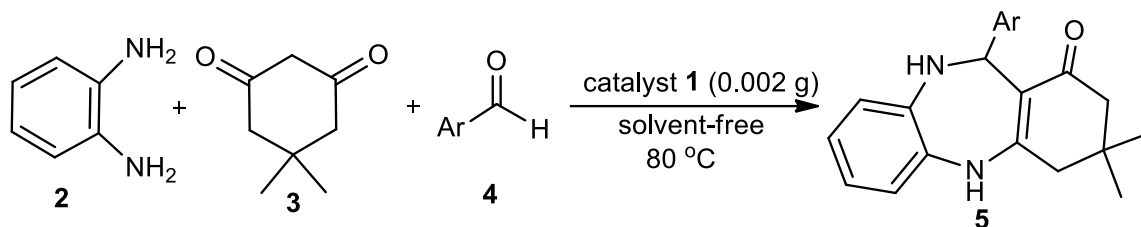
Scheme-2. Synthesis of 4-substituted-1,5-benzodiazepines using $\text{Fe}_3\text{O}_4@\text{TiO}_2\text{-H}_5\text{IO}_6$.

Table-1: Evaluating reaction conditions on the model reaction.

Entry	Solvent	Catalyst loading	T (°C)	Time/Yield ^a (min/%)
1	-	-	25	360/0
2	-	-	70	360/10
3	-	Cat 1 (0.001 g)	70	30/60
4	-	Cat 1 (0.002 g)	70	30/80
5	-	Cat 1 (0.003 g)	70	30/80
6	-	Cat 1 (0.004 g)	70	30/65
7	-	Cat 1 (0.002 g)	80	10/95
8	-	Cat 1 (0.002 g)	90	10/90
9	-	Cat 1 (0.002 g)	100	10/85
10	-	Cat 1 (0.002 g)	110	10/75
11	EtOH	Cat 1 (0.002 g)	reflux	30/60
12	H ₂ O	Cat 1 (0.002 g)	reflux	30/50
13	CHCl ₃	Cat 1 (0.002 g)	reflux	30/65
14	THF	Cat 1 (0.002 g)	reflux	30/70
15	-	H ₅ IO ₆ (2 mol%)	80	100/60
16	-	H ₅ IO ₆ (5 mol%)	80	100/65
17	-	H ₅ IO ₆ (10 mol%)	80	100/70

^aIsolated yields.Table-2: Preparation of 4-substituted-1,5-benzodiazepine derivatives by using $\text{Fe}_3\text{O}_4@\text{TiO}_2\text{-H}_5\text{IO}_6$.^a

Entry	Ar	Time (min)	Yield ^b (%)	Mp (°C)
5a	C ₆ H ₅	10	95	248-250 ¹⁹
5b	4-NO ₂ C ₆ H ₄	7	95	272-274 ⁶⁴
5c	4-ClC ₆ H ₄	7	95	238-241 ⁴
5d	4-OHC ₆ H ₄	10	92	229-232 ⁴
5e	4-CH ₃ C ₆ H ₄	8	90	223-225 ¹⁹
5f	3-ClC ₆ H ₄	7	95	230-231 ¹
5g	3-NO ₂ C ₆ H ₄	7	96	146-147 ⁴
5h	4-BrC ₆ H ₄	7	93	222-224 ⁶⁵
5i	4-CH ₃ OC ₆ H ₄	8	94	249-250 ⁴
5j	4-Cl-5-NO ₂ C ₆ H ₃	7	90	195-196 ⁶⁶
5k	2-Thionyl	10	90	264-266 ¹
5l	4-Br-2-OHC ₆ H ₃	7	96	278-280 ^c

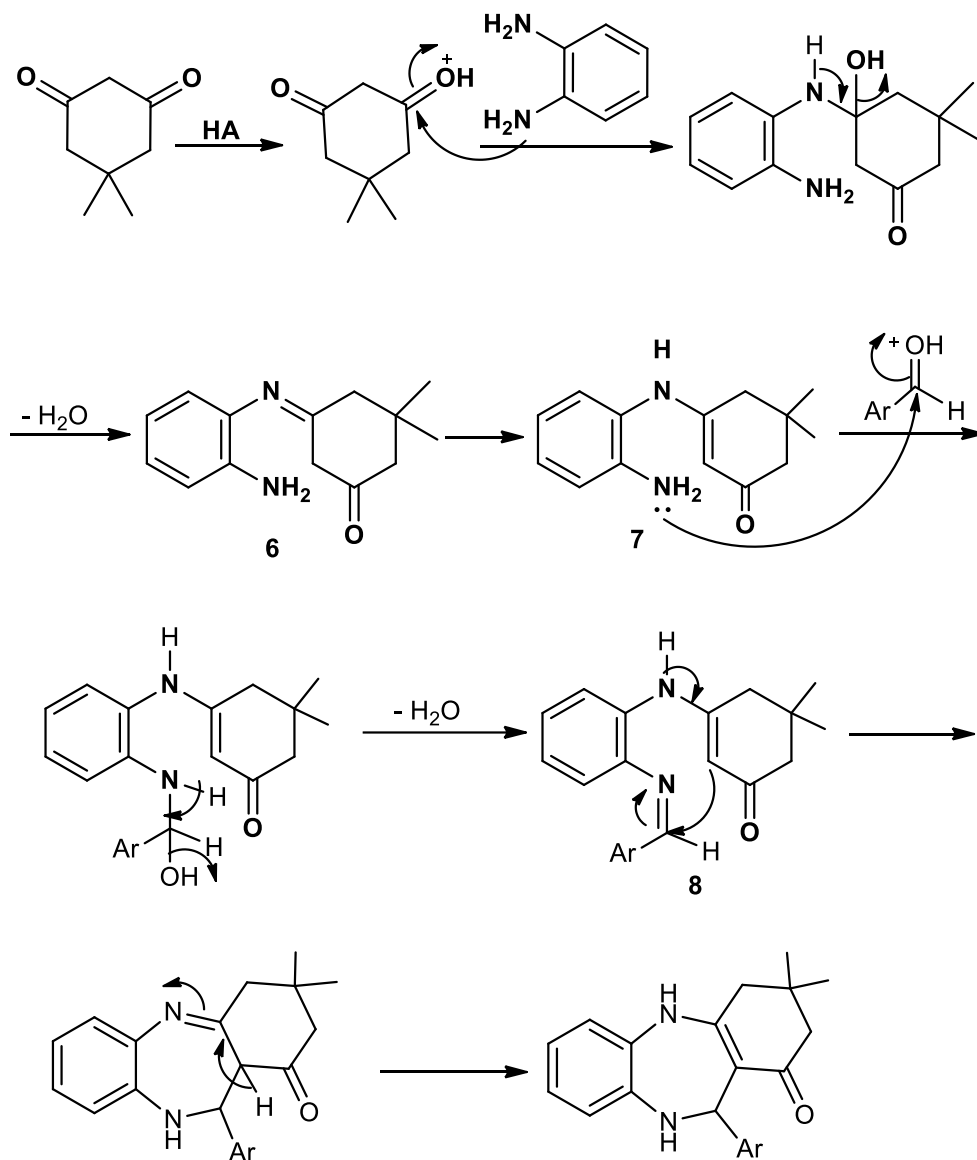
^aReaction condition: aldehyde (1 mmol), *o*-phenylenediamine (1 mmol), dimedone (1 mmol) and catalyst **1** (0.002 g) at 80 °C. ^bIsolated yields. ^cNovel compound.

In determining optimal conditions, some of the 4-substituted-1,5-benzodiazepine derivatives were prepared in the presence of different aldehydes, having both types of substituent electron-donating and electron-withdrawing. According to the proposed mechanism, the results demonstrate electron-withdrawing functional groups various positions, especially in para-substituted aromatic aldehydes, have shorter reaction times and higher efficiency. But in general, in all substituted aromatic, the reaction time is short, and the efficiency is excellent, as stated in the references^{1,4,19}, which shows the best and effective performance of $\text{Fe}_3\text{O}_4@\text{TiO}_2\text{-H}_5\text{IO}_6$ as a catalyst in preparing 1,5-benzodiazepines (Table-2).

According to the reported mechanisms in the literature [4], we proposed a probable mechanism for

the preparation of 4-substituted-1,5-benzodiazepines **5** by using the acidic catalyst **1** (Scheme 3). Initially, the NH₂ group of *o*-phenylenediamine attacks/ the activated carbonyl group of dimedone to give intermediate **6**. In the following, imine **6** performs a 1,3-hydrogen shift to produce enamine **7**. The amino group of **7** reacts with the carbonyl group of aldehyde to form intermediate **8**. Finally, the seven-membered ring benzodiazepine is obtained by the intramolecular cyclization of adduct **8**.

As exhibited in Table-3, the most important benefits of the current protocol over the presented methods can be understandable just by comparison of our outcomes with those of lately published pathways.



HA: $\text{Fe}_3\text{O}_4@\text{TiO}_2\text{-H}_5\text{IO}_6$

Scheme-3. The suggested mechanism for synthesizing of **5** by $\text{Fe}_3\text{O}_4@\text{TiO}_2\text{-H}_5\text{IO}_6$.

Table-3: Comparison of the results for the preparation of compound **5b** with various used catalysts.

Catalyst	Conditions	Time (min)	Yield ^a (%)
Sulfated polyborate (10 mol%)	solvent-free, 100 °C	10	98 ¹
ZnS Nanoparticles (0.01 g)	EtOH, reflux	8	94 ¹⁹
La_2O_3 (1 mol%)	solvent-free, 60 °C	210	83 ⁶⁷
$\text{La}(\text{OH})_3$ (1 mol%)	solvent-free, 60 °C	180	85 ⁶⁸
$\text{Fe}_3\text{O}_4@\text{TiO}_2\text{-H}_5\text{IO}_6$ (0.002 g)	solvent-free, 80 °C	7	95

^aIsolated yields.

To investigate any leaching of H_5IO_6 from the $\text{Fe}_3\text{O}_4@\text{TiO}_2\text{-H}_5\text{IO}_6$ solid acid catalyst, we have performed an in situ filtration technique. When the reaction progress reached 50%, warm acetonitrile (5 mL) was added, and the catalyst isolation was carried

out by simple filtration. After removing the solvent, the catalyst-free residue continued the process under the conditions which before were optimized. As we expected, the progress of the reaction stopped, which confirms that no leaching of the supported catalytic

centers has happened under optimized conditions. Furthermore, the reusability of $\text{Fe}_3\text{O}_4@\text{TiO}_2\text{-H}_5\text{IO}_6$ was investigated in the model reaction. After completion of the reaction, acetonitrile (5 mL) was added to the mixture, and the catalyst was filtered, washed with EtOH (10 mL), and deionized water (10 mL), followed by drying at 100 °C. Applying the recovered catalyst for six successive runs in the model reaction generated the product, having a negligible reduction in yield (Fig. 6). As seen, establishing the fact that the $\text{Fe}_3\text{O}_4@\text{TiO}_2\text{-H}_5\text{IO}_6$ catalyst possesses recycling ability with no significant decrease in its activity.



Fig. 6: Reusability of $\text{Fe}_3\text{O}_4@\text{TiO}_2\text{-H}_5\text{IO}_6$ in the reaction of benzaldehyde, *o*-phenylenediamine, and dimedone.

Conclusions

In this work, for the first time, TiO_2 coated Fe_3O_4 was functionalized by periodic acid, and it was utilized as a new, efficient and reusable magnetic nanocatalyst for the synthesis of benzodiazepine derivatives. This new catalytic system demonstrated the advantages of environmentally benign character, quickly separation, non-toxicity, mild reaction conditions, short reaction times, and good reusability.

Acknowledgements

The authors gratefully acknowledge partial support of this work by Yasouj University, Yasouj, Iran.

References

1. K. S. Indalkar, M. S. Patil and G. U. Chaturbhuj, An efficient, environmentally benign, and solvent-free protocol for the synthesis of 4-substituted 1,5-benzodiazepines catalyzed by

- reusable sulfated polyborate, *Tetrahedron Lett.*, **58**, 4496 (2017).
2. E. C. Cortes, L. V. C. Ana and G. M. Olivia, New derivatives of dibenzo[b,e][1,4]diazepin-1-ones by an efficient synthesis and spectroscopy, *J. Heterocycl. Chem.*, **44**, 183 (2007).
3. L. Makaron, C. A. Moran, O. Namjoshi, S. Rallapalli, J. M. Cook and J. K. Rowlett, Cognition-impairing effects of benzodiazepine-type drugs: role of GABAA receptor subtypes in an executive function task in rhesus monkeys, *Pharmacol. Biochem. Behav.*, **104**, 62 (2013).
4. A. Savari, F. Heidarzadeh and N. Pourreza, Synthesis and characterization of $\text{CoFe}_2\text{O}_4@\text{SiO}_2@\text{NH-NH}_2\text{-PCuW}$ as an acidic nanocatalyst for the synthesis of 1,4-benzodiazepines and a powerful dye remover, *Polyhedron*, **166**, 233 (2019).
5. R. Kumar and Y. C. Joshi, Synthesis and antimicrobial, antifungal and anthelmintic activities of 3*H*-1,5-benzodiazepine derivatives, *J. Serb. Chem. Soc.*, **73**, 937 (2008).
6. A. M. Holbrook, R. Crowther, A. Lotter, C. Cheng and D. King, Meta-analysis of benzodiazepine use in the treatment of insomnia, *Can. Med. Assoc. J.*, **162**, 225 (2000).
7. C. L. Zhang, S. S. Chatterjee, U. Stein and U. Heinemann, Comparison of the effects of losigamone and its isomers on maximal electroshock induced convulsions in mice and on three different patterns of low magnesium induced epileptiform activity in slices of the rat temporal cortex, *Naunyn. Schmiedeberg's Arch. Pharmacol.*, **345**, 85 (1992).
8. X. Q. Pan, J. P. Zou, Z. H. Huang and W. Zhang, $\text{Ga}(\text{OTf})_3$ -promoted condensation reactions for 1,5-benzodiazepines and 1,5-benzothiazepines, *Tetrahedron Lett.*, **49**, 5302 (2008).
9. S. V. Ley, M. L. Trudell and D. J. Wadsworth, The total synthesis of agglomerin A and (\pm)-carolinic acid. A general method for the preparation of 3-acyl tetronic acids via direct acylation of *o*-methyl 3-stannyl tetronates, *Tetrahedron*, **47**, 8285 (1991).
10. M. Matsumoto, Y. Kawamura, Y. Yoshimura, Y. Terui, H. Nakai, T. Yoshida and J. I. Shoji, Isolation, characterization and structures of PA-46101 A and B, *J. Antibiot.*, **43**, 739 (1990).
11. J. I. Schimer, P. Cigler, J. Vesely, K. R. Grantz Saskova, M. Lepsik, J. I. Brynda, P. N. Rezacova, M. Kozicek, I. Cisarova and H. Oberwinkler, Structure-aided design of novel inhibitors of HIV protease based on a benzodiazepine scaffold, *J. Med. Chem.*, **55**, 10130 (2012).
12. L. D. Fader, R. Bethell, P. Bonneau, M. Bös, Y. Bousquet, M. G. Cordingley, R. Coulombe, P.

- Deroy, A. M. Faucher and A. Gagnon, Discovery of a 1,5-dihydrobenzo [b][1,4] diazepine-2,4-dione series of inhibitors of HIV-1 capsid assembly, *Bioorg. Med. Chem. Lett.*, **21**, 398 (2011).
13. H. A. Wieland, H. Luddens and P. H. Seeburg, A single histidine in GABAA receptors is essential for benzodiazepine agonist binding, *J. Biol. Chem.*, **267**, 1426 (1992).
 14. H. Shaabani, A. Maleki and H. Mofakham, Novel multicomponent one-pot synthesis of tetrahydro-1H-1,5-benzodiazepine-2-carboxamide derivatives, *J. Comb. Chem.*, **10**, 595 (2008).
 15. A. M. El-Snyed, H. Abdel-Ghany and A. M. M. El-Sngnier, A Novel Synthesis of pyrano(2,3-*c*)-,1,3-oxazino (2,3*b*)-,1,2,4-triazolo(3,4-*b*)-,oxazolo(2,3-*b*)-,furano(3,2-*c*)-, and 3-substituted-(1,5)benzodiazepin-2-ones, *Synth. Commun.*, **29**, 3561 (1999).
 16. M. Curini, F. Epifano, M. C. Marcotullio and O. Rosati, Ytterbium triflate promoted synthesis of 1,5-benzodiazepine derivatives, *Tetrahedron Lett.*, **42**, 3193 (2001).
 17. R. Varala, R. Enugala, S. Nuvula and S. R. Adapa, Ceric ammonium nitrate (CAN) promoted efficient synthesis of 1,5-benzodiazepine derivatives, *Synlett*, **2006**, 1009 (2006).
 18. Z. Nasir, A. Ali, M. Shakir, R. Wahab, S. Uzzaman and L. Fullah, Silica-supported NiO nanocomposites prepared via a sol-gel technique and their excellent catalytic performance for one-pot multicomponent synthesis of benzodiazepine derivatives under microwave irradiation, *New J. Chem.*, **41**, 5893 (2017).
 19. H. Naeimi and H. Foroughi, ZnS nanoparticles as an efficient recyclable heterogeneous catalyst for one-pot synthesis of 4-substituted-1,5-benzodiazepines, *New J. Chem.*, **39**, 1228 (2015).
 20. M. Ghandi, T. Momeni and M. T. Nazeri, N. Zarezadeh and M. Kubicki, A one-pot three-component reaction providing tricyclic 1,4-benzoxazepine derivatives, *Tetrahedron Lett.*, **54**, 2983 (2013).
 21. K. Murai and R. Nakatani, One-pot three-component reaction providing 1,5-benzodiazepine derivatives, *Tetrahedron*, **64**, 11034 (2008).
 22. B. Karami, M. Kiani, S. J. Hosseini and M. Bahrami, Synthesis and characterization of novel nanosilica molybdic acid and its first catalytic application in the synthesis of new and known pyranocoumarins, *New J. Chem.*, **39**, 8576 (2015).
 23. H. Bienayme, C. Hulme, G. Odon and P. Schmitt, Maximizing synthetic efficiency: Multi-component transformations lead the way, *Chem. Eur. J.*, **6**, 3321 (2000).
 24. J. Liu, A. Plog, P. Groszewicz, L. Zhao, Y. Xu, H. Breitzke, A. Stark, R. Hoffmann, T. Gutmann and K. Zhang, Design of a heterogeneous catalyst based on cellulose nanocrystals for cyclopropanation: Synthesis and solid-state NMR characterization, *Chem. Eur. J.*, **21**, 12414 (2015).
 25. M. H. Valkenberg and W. F. Holderich, Preparation and use of hybrid organic-inorganic catalysts, *Catal. Rev.*, **44**, 321 (2002)
 26. L. Z. Fekri, M. Nikpassand, S. Pourmirzajani and B. Aghazadeh, Synthesis and characterization of amino glucose-functionalized silica-coated NiFe₂O₄ nanoparticles: A heterogeneous, new and magnetically separable catalyst for the solvent-free synthesis of pyrano[3,2-*c*]chromen-5(4*H*)-ones, *RSC Adv.*, **8**, 22313 (2018).
 27. B. Karami, M. Farahi, N. Farmani and H. Mohamadi Tanuraghaj, Novel synthesis of coumarin-containing secondary benzamide derivatives using tungstate sulfuric acid, *New J. Chem.*, **40**, 1715 (2016).
 28. N. Ahmad and Z. Siddiqui, Sulphated silica tungstic acid as a highly efficient and recyclable solid acid catalyst for the synthesis of tetrahydropyrimidines and dihydropyrimidines, *J. Mol. Catal. A: Chem.*, **387**, 45 (2014).
 29. S. Sharma, P. Parikh and R. Jasra, Reconstructed Mg/Al hydrotalcite as a solid base catalyst for synthesis of jasminaldehyde, *Appl. Catal., A*, **386**, 34 (2010).
 30. E. Kolvari, N. Koukabi and M. Hosseini, Perlite: A cheap natural support for immobilization of sulfonic acid as a heterogeneous solid acid catalyst for the heterocyclic multicomponent reaction, *J. Mol. Catal. A: Chem.*, **397**, 68 (2015).
 31. S. Ghodke and U. Chudasama, Solvent free synthesis of coumarins using environment friendly solid acid catalysts, *Appl. Catal. A*, **453**, 219 (2013).
 32. Y. Xu, X. Shi, R. Hua, R. Zhang, Y. Yao, B. Zhao, T. Liu, J. Zheng and G. Lu, Remarkably catalytic activity in reduction of 4-nitrophenol and methylene blue by Fe₃O₄@COF supported noble metal nanoparticles, *Appl. Catal. B*, **260**, 118142 (2020).
 33. S. Neumann, H. Hannes Doebler, S. Keil, A. J. Erdt, C. Gutsche, H. Borchert, J. Kolny-Olesiak, J. Parisi, M. Baumer and S. Kunz, Effects of particle size on strong metal-support interactions using colloidal “surfactant-free” Pt nanoparticles supported on Fe₃O₄, *ACS Catal.*, **10**, 4136 (2020).
 34. S. Ikeda, S. Ishino, T. Harada, N. Okamoto, T. Sakata, H. Mori, S. Kuwabata, T. Torimoto and M. Matsumura, Ligand-free platinum nanoparticles encapsulated in a hollow porous carbon shell as a highly active heterogeneous

- hydrogenation catalyst, *Angew. Chem.*, **118**, 7221 (2006).
35. J. Rahimi, R. Taheri-Ledari, M. Niksefat and A. Maleki, Enhanced reduction of nitrobenzene derivatives: Effective strategy executed by Fe₃O₄/PVA-10% Ag as a versatile hybrid nanocatalyst, *Catal. Commun.*, **134**, 105850 (2020).
 36. X. Wang, F. Pan, Zh. Xiang, Q. Zeng, K. Pei, R. Che and W. Lu, Magnetic vortex core-shell Fe₃O₄@C nanorings with enhanced microwave absorption performance, *Carbon*, **157**, 130 (2020).
 37. R. Taheri-Ledari, A. Maleki, E. Zolfaghari, M. Radmanesh, H. Rabbani, A. Salimi and R. Fazel, High-performance sono/nano-catalytic system: Fe₃O₄@Pd/CaCO₃-DTT core/shell nanostructures, a suitable alternative for traditional reducing agents for antibodies, *Ultrason. Sonochem.*, **61**, 104824 (2020).
 38. H. Veisi, T. Ozturk, B. Karmakar, T. Tamoradi and S. Hemmati, In situ decorated Pd NPs on chitosan-encapsulated Fe₃O₄/SiO₂-NH₂ as magnetic catalyst in Suzuki-Miyaura coupling and 4-nitrophenol reduction, *Carbohydr. Polym.*, **235**, 115966 (2020).
 39. S. Kamari and A. Shahbazi, Biocompatible Fe₃O₄@SiO₂-NH₂ nanocomposite as a green nanofiller embedded in PES-nanofiltration membrane matrix for salts, heavy metal ion and dye removal: Long-term operation and reusability tests, *Chemosphere*, **243**, 125282 (2020).
 40. Y. Yang, B. Xu, J. He, J. Shi, L. Yud and Y. Fan, Design and synthesis of Fe₃O₄@SiO₂@mSiO₂-Fe: A magnetically separable catalyst for selective oxidative cracking reaction of styrene using air as partial oxidant, *Appl. Catal. A*, **590**, 117353 (2020).
 41. F. Rezaei, M. A. Amrollahi and R. Khalifeh, Brønsted acidic dicationic ionic liquid immobilized on Fe₃O₄@SiO₂ nanoparticles as an efficient and magnetically separable catalyst for the synthesis of bispyrazoles, *ChemistrySelect*, **5**, 1760 (2020).
 42. S. Xuan, W. Jiang, X. Gong, Y. Hu and Z. Chen, Magnetically separable Fe₃O₄/TiO₂ hollow spheres: Fabrication and photocatalytic activity, *J. Phys. Chem. C*, **113**, 553 (2009).
 43. J. Liu, J. Xu, R. Che, H. Chen, M. Liu and Z. Liu, Hierarchical Fe₃O₄@TiO₂ yolk-shell microspheres with enhanced microwave-absorption properties, *Chem. Eur. J.*, **19**, 6746 (2013).
 44. A. Liu, H. Zhang, J. Ding, W. Kou, F. Yan, K. Huang and H. Chen, Enrichment of phospholipids using magnetic Fe₃O₄/TiO₂ nanoparticles for quantitative detection at single cell levels by electrospray ionization mass spectrometry, *Talanta*, **212**, 120769 (2020).
 45. Y. Yao, S. Miao, S. Liu, L. P. Ma, H. Sun and S. Wang, Synthesis, characterization, and adsorption properties of magnetic Fe₃O₄@graphene nanocomposite, *Chem. Eng. J.*, **184**, 326 (2012).
 46. L. Qi, R. Xu and J. Gong, Monitoring DNA adducts in human blood samples using magnetic Fe₃O₄@graphene oxide as a nano-adsorbent and mass spectrometry, *Talanta*, **209**, 120523 (2020).
 47. B. Karami, S. J. Hoseini, K. Eskandari, A. Ghasemi and H. Nasrabadi, Synthesis of xanthene derivatives by employing Fe₃O₄ nanoparticles as an effective and magnetically recoverable catalyst in water. *Catal. Sci. Technol.*, **2**, 331 (2012).
 48. B. Karami, V. Ghashghaee and S. Khodabakhshi, Novel silica tungstic acid (STA): Preparation, characterization and its first catalytic application in synthesis of new benzimidazoles, *Catal. Commun.*, **20**, 70 (2012).
 49. S. Khodabakhshi and B. Karami, A rapid and eco-friendly synthesis of novel and known benzopyrazines using silica tungstic acid (STA) as a new and recyclable catalyst, *Catal. Sci. Technol.*, **2**, 1940 (2012).
 50. B. Karami, S. Khodabakhshi and F. Hashemi, Synthesis of a novel class of benzofurans via a three-component, regiospecific intramolecular heterocyclization reaction, *Tetrahedron Lett.*, **54**, 3583 (2013).
 51. B. Karami, M. Farahi, S. Akrami and D. Elhamifar, Tungstic acid-functionalized MCM-41 as a novel mesoporous solid acid catalyst for the one-pot synthesis of new pyrrolo[2,1-a]isoquinolines. *New J. Chem.*, **42**, 12811 (2018).
 52. K. Eskandari and B. Karami, A nanocatalyst-assisted protocol to the synthesis of bis(pyrazolyl)methane derivatives bearing aroyl groups by the use of arylglyoxals in the presence of ZnO nanowires as a highly efficient, recyclable, and green catalyst. *Can. J. Chem.*, **96**, 377 (2018).
 53. S. Akrami, B. Karami and M. Farahi, Preparation and characterization of novel phthalhydrazide-functionalized MCM-41 and its application in the one-pot synthesis of coumarin-fused triazolopyrimidines, *RSC Adv.*, **7**, 34315 (2017).
 54. M. Farahi, B. Karami, Z. Banaki, F. Rastgoo and K. Eskandari, TSA-catalyzed regioselective synthesis of medicinally important 4-aryl-substituted dihydropyrimidine derivatives fused to pyrazole and triazole scaffolds via an efficient and green domino reaction, *Monatsh. Chem.*, **148**, 1469 (2017).

55. B. Karami and M. Kiani, Application of 7-amino coumarins for the synthesis of novel and thermally stable water-insoluble azo-coumarin dyes, *J. Iran. Chem. Soc.*, **13**, 111 (2016).
56. S. Khodabakhshi, B. Karami, K. Eskandari, S. J. Hoseini and H. Nasrabadi, Convenient on water synthesis of novel derivatives of dicoumarol as functional vitamin K depleter by Fe₃O₄ magnetic nanoparticles, *Arab. J. Chem.*, **10**, S3907 (2017).
57. S. Akrami, B. Karami and M. Farahi, A novel protocol for catalyst-free synthesis of fused six-member rings to triazole and pyrazole, *Mol. Divers.*, **24**, 225 (2020).
58. M. Farahi, B. Karami, R. Keshavarz and F. Khosravian, Nano-Fe₃O₄@SiO₂-supported boron sulfonic acid as a novel magnetically heterogeneous catalyst for the synthesis of pyranocoumarins, *RSC Adv.*, **7**, 46644 (2017).
59. F. Khosravian, B. Karami and M. Farahi, Synthesis and characterization of molybdic acid immobilized on modified magnetic nanoparticles as a new and recyclable catalyst for the synthesis of chromeno[4,3-*b*]chromenes, *New J. Chem.*, **41**, 11584 (2017).
60. J. Etemad Gholtash and M. Farahi, Tungstic acid-functionalized Fe₃O₄@TiO₂: Preparation, characterization and its application for the synthesis of pyrano[2,3-*c*]pyrazole derivatives as a reusable magnetic nanocatalyst, *RSC Adv.*, **8**, 40962 (2018).
61. Y. Wei, B. Han, X. Hu, Y. Lin, X. Wang and X. Deng, Synthesis of Fe₃O₄ nanoparticles and their magnetic properties, *Procedia Engin.*, **27**, 632 (2012).
62. U. C. Rajesh and D. S. Rawat, Functionalized superparamagnetic Fe₃O₄ as an efficient quasi-homogeneous catalyst for multi-component reactions, *RSC Adv.*, **4**, 41323 (2014).
63. N. K. Cakmak, Z. Said, L. S. Sundar, Z. M. Ali and A. K. Tiwari, Preparation, characterization, stability, and thermal conductivity of rGO-Fe₃O₄-TiO₂ hybrid nanofluid: An experimental study, *Powder Technol.*, **372**, 235 (2020).
64. L. Z. Fekri, S. Sarhandi and E. Vessally, Ultrasound assisted 1,4-diazabicyclo[2.2.2]octaniumdiacetate multicomponent synthesis of benzodiazepines: A novel, highly efficient and green protocol, *Acta Chim. Slov.*, **65**, 246 (2018).
65. N. S. Miri and J. Safaei-Ghomi, Synthesis of benzodiazepines catalyzed by CoFe₂O₄@SiO₂-PrNH₂ nanoparticles as a reusable catalyst, *Z. Naturforsch.*, **72**, 497 (2017).
66. H. Naeimi and H. Foroughi, Efficient, environmentally benign, one-pot procedure for the synthesis of 1,5-benzodiazepine derivatives using *N*-methyl-2-pyrrolidonium hydrogen sulphate as an ionic liquid catalyst under solvent-free conditions, *Chin. J. Catal.*, **36**, 734 (2015).
67. D. Nandan, S. K. Saxena and N. Viswanadham, Synthesis of hierarchical ZSM-5 using glucose as a templating precursor, *J. Mater. Chem. A*, **2**, 1054 (2014).